Arabian Journal of Chemistry (2021) **14**, 103241

King Saud University

Arabian Journal of Chemistry

www.ksu.edu.sa
www.sciencedirect.com

ORIGINAL ARTICLE

Development of lactobionic acid conjugated-copper chelators as anticancer candidates for hepatocellular carcinoma

Xueke Zhao [a,1], Xiang Li [b,c,1], Xiaoping Huang [c], Shuyu Liang [b], Penggen Cai [a], Yuhui Wang [c], Yongming Cui [a], Wu Chen [a], Xiongwei Dong [a,*]

[a] *National Local Joint Engineering Laboratory for Advanced Textile Processing and Clean Production, Wuhan Textile University, Wuhan 430073, Hubei, PR China*
[b] *College of Chemistry and Molecular Engineering, Peking University, Beijing, 100871 Beijing, PR China*
[c] *School of Chemistry, Central China Normal University, Wuhan 430079, Hubei, PR China*

Received 17 April 2021; accepted 28 May 2021
Available online 11 June 2021

KEYWORDS

Copper chelation;
Hepatocellular carcinoma;
Copper deposition;
Apoptosis;
Hepatic targeting

Abstract Hepatic copper deposition leads to metabolic disorders, rapid increase in reactive oxygen species (ROS) levels, and even the occurrence and metastasis of hepatocellular carcinoma. Copper chelation or copper transporter inhibition have already been developed into an effective method to control the canceration of hepatocytes and kill the hepatocarcinoma cells. Here, we designed three novel lactobionic acid conjugated copper chelators (**GT1, 9** and **10**), which have the potential to be recognized by asialoglycoprotein receptor (ASGPR), a high-capacity C-type lectin receptor selectively expressed in liver. Both **GT1, 9** and **10** can selectively and efficiently coordinate with copper in solution and in the high-copper treated hepatocellular carcinomas model **(HC HepG2** cells). The thiosemicarbazone-based chelator **GT1** should more effectively eliminate copper and promote apoptosis of **HC HepG2** cells, which might have application prospects in preventing cancerization and other pathological lesions caused by copper deposition of liver. Moreover, our results also revealed the potential of **GT1** to be harnessed as preventive leading structures of the hepatocellular carcinomas.

1. Introduction

Copper, a redox active metal ion, is essential for most organisms, which serves as cofactor for various enzymes and regulates energy generation, oxygen transport, cellular metabolism, signal transduction, and other biochemical processes (Kim et al., 2008). In the organism, copper accumulation is associated with cellular and apoptotic injury (Johncilla and

* Corresponding author.
E-mail address: xwdong@wtu.edu.cn (X. Dong).
[1] The work has been contributed by these authors equally.

Peer review under responsibility of King Saud University.

Production and hosting by Elsevier

https://doi.org/10.1016/j.arabjc.2021.103241

Mitchell, 2011), and copper deficiency will cause severe malnutrition, chronic diarrhea, and genetic diseases (Williams, 1983). Therefore, cellular copper concentrations must be maintained somewhere below toxicity and above nutrient deficiency (Kim et al., 2008; Harris, 2001). Disruption of copper homeostasis in the organisms is closely related to the occurrence and development of many diseases, such as Alzheimer's disease, Wilson's disease, prion diseases, carcinogenesis, and so on (Członkowska et al., 2018; Daniel et al., 2004; Stepien et al., 2017; Bandmann et al., 2015).

Liver is the key organ in the supply, storage, and excretion of copper, in which copper can be used for protein and energy production (Roberts and Sarkar, 2008). Catalytic copper, because of its redox activity and mobilization, introduce the formation of reactive oxygen species (ROS) through Haber-Weiss-like reactions, which gives rise to fast DNA damage and also leads to carcinogenesis (Zubair et al., 2013; Aruoma et al., 1991; Theophanides and Anastassopoulou, 2002). A large number of clinical and experimental evidences indicate that copper deposition in the liver should lead to a variety of serious diseases, especially the hepatocellular carcinoma (Theophanides and Anastassopoulou, 2002; Smallwood et al., 1968; Wooton-Kee et al., 2015; Danks, 1991). Copper deposition leads to the ROS production, which makes liver cells proliferate abnormally and activate oncogenes. On the other hand, liver metabolic disorders caused by copper deposition also further increase the copper level in the liver, causing a vicious circle (Hussain et al., 2007, 2003; Merlot et al., 2013; Paulsen and Carroll, 2013).

The rapid proliferation, invasion and metastasis of hepatocarcinoma cells always depend on high levels of copper (Chandan et al., 2018; Bruix et al., 2004; Ueda et al., 1993). Intracellular copper is required for oncogenic BRAF signaling, tumorigenesis and activation of the mitogen-activated protein kinase (MAPK) pathway (Turski et al., 2012; Brady et al., 2014). Because copper accumulation is important for the cancerization and deterioration of the liver, chelating copper ions or inhibiting the activity of copper transporters have already become effective intervention methods for hepatocellular carcinoma (Brady et al., 2014; Wang et al., 2015; Krasnovskaya et al., 2016; Kacar et al., 2020; Yoshii et al., 2001; Porchia et al., 2020; Gupte and Mumper, 2009; Santini et al., 2014; Safi et al., 2014). Previously, Peter J. Crouch and the collaborators had developed a highly effective copper chelator **GTSM**, glyoxalbis(N(4)-methylthiosemicarbazonato), which achieved intracellular copper chelation, transport and re-release, and increased intracellular copper bioavailability (Crouch et al., 2009). Referring to the coordination mechanism of **GTSM** with copper, we are expected to design novel chelators to eliminate copper deposition and biologically reuse the excessive copper in the liver, and ultimately achieve the intervention and treatment of copper-dependent hepatocellular carcinoma.

In order to develop copper chelators for hepatocyte-specific targeting, we can utilize asialoglycoprotein receptor (ASGPR), a high-capacity C-type lectin receptor selectively expressed on mammalian hepatocytes, which recognizes N-acetylgalactosamine and galactose-containing glycopeptide substrates (Rigopoulou et al., 2012). Hitherto, conjugating drugs with galactose or its glycomimetic have developed into an effective strategy for hepatocyte-targeted drug delivery *via* ASGPR (Mamidyala et al., 2012; Huang et al., 2017; Bernardes et al., 2010; Pujol et al., 2011; Sanhueza et al., 2017). Besides, the capacity of ASGPR to import molecules across the cellular plasma membrane also makes it an enticing target for delivery to hepatocellular carcinomas system *via* ASGPR-mediated endocytosis (Li et al., 2008).

Here, based on the copper coordination chemistry and the selective recognition mechanism of ASGPR, three novel hepatocyte-targeted copper chelators were designed by combining phenol, thiosemicarbazone or semicarbazone, and lactobionic acid. Comparing with semicarbazone-based chelators **GT9** and **GT10**, the thiosemicarbazone-based chelator **GT1** has stronger binding ability to copper, and can more effectively chelate copper ions in solution and in high-copper treated hepatocellular carcinomas model (**HC HepG2** cells). The lethal concentration of **GT1** to **HC HepG2** cells approach micro-molar levels, and 5 μM **GT1** can effectively promote apoptosis and kill **HC HepG2** cells. Furthermore, our results also indicated that **GT1** has the proper binding capacity to copper ions ($\log K^{2+}_{Cu} = 17.48 \pm 0.11$), and so will not interfere with the function of copper-containing proteins and enzymes, such as copper/zinc superoxide dismutase (SOD1). Thus, this study established the power of **GT1** in the killing of copper-deposited hepatocellular carcinomas and in the removing of copper ions from liver cells.

2. Experimental section

2.1. Materials and instrumentation

Unless otherwise noted, materials were purchased from commercial suppliers and used without further purification. All the solvents were treated according to standard methods. DMEM, FBS, 0.25% trypsin-EDTA, penicillin, streptomycin and PBS were purchased from Gibco Inc (Gibco, USA). UV–vis spectra were recorded on an Analytik Jena Specord 210 spectrophotometer (Analytic Jena AG). ^{1}H NMR spectra were recorded on a Varian Mercury 600 spectrometer. Data are reported as follows: chemical shift, multiplicity (s = singlet, d = doublet, t = triplet, dd = doublet of doublets, m = multiplet), coupling constants (Hz) and integration. The MS data were obtained using a Quattro II ESI mass spectrometer (Waters, USA). The data of flow cytometry were performed on BD flow cytometer (BD, USA). Potentiometric titrations were performed with a Metrohm 877 Titrino Plus automated titrator equipped with a Metrohm 6.0262.100 glass electrode calibrated against standard buffers. Elementary analysis was carried out on a PerkinElmer 2400 analyser (PerkinElmer, USA). FTIR spectra were recorded on a Bruker Vertex 70 device (Bruker, Germany) using KBr pellets.

2.2. Determination of acidity and stability constants

Acidity constants (pKa) of the chelators and stability constant (pK) of the M^{2+}-complexes (M = Cu, Zn, Mn and Fe) were determined by potentiometric titrations. The water-jacketed titration vessel was maintained at 25.0 °C (±0.5 °C). To estimate pKa values, chelators were predissolved in an excess of HCl (1.0 mM) and diluted with water [10% (vol/vol) DMSO] in the titration vessel (25.0 mL), the final concentrations of HCl and chelators were 100 μM. All measurements were conducted in the presence of 100 mM KCl to maintain constant

ionic strength. Solutions were titrated with 75.5 mM NaOH, which was prepared with degassed water and standardized with Potassium biphthalate prior to each titration. Data analysis was carried out with the program HyperQuad 2013 (Protonic Software, UK) (Gans et al., 1999, 1996). Stability constant of M^{2+}-complex was determined by the titrations performed in the presence of 1.0 equiv of 100.0 μM metal nitrates using the pK_a values determined above. Species distribution plots and titration simulations were built with the program HySS2009 (Protonic Software) (Thomas et al., 1979; Alderighi et al., 1999). The data represented here were the mean ± SD of the results obtained from at least three independent measurements.

2.3. Cell culture

HepG2, HeLa and MCF-7 cells were cultured in culture media (DMEM supplemented with 10% FBS, 50 unit/mL of penicillin, and 50 μg/mL of streptomycin). MCF-10A cells were cultured in CM-0525 culture media (Procell, China). All cells were cultured under standard conditions (37 °C, 5% CO_2, 100% humidity) with weekly passaging. Culture media were replaced with fresh media every day.

2.4. Intracellular copper detection by flow cytometry

The cells were seeded in a 6-well plate at a density of 10^4 cells per mL in culture media. After 24 h, the cells were treated without or with Cu^{2+} in culture media for 48 h at 37 °C. After washing with PBS, the cells were further incubated without or with chelators in culture media for 24 h at 37 °C. Because DMSO was used as a co-solvent for chelator, the same amount of DMSO (5‰) was added as a control group. In other subsequent intracellular experiments, we also used DMSO (5‰) as a control group. Then, the cells were washed three times with PBS and incubated with 5 μM Cu^{2+} fluorescent probe (Rhodamine 6G hydrazide) for another 1 h. Finally, cells were washed by PBS, dissociated by 0.25% trypsin-EDTA and re-suspended in PBS. Fluorescence data was collected and analyzed on the BD flow cytometry.

2.5. Cell apoptosis assay

FITC-conjugated annexin-V assays were used to assess cell apoptosis. Following the manufacturer's instructions of Annexin V-FITC Apoptosis Detection Kit (Abcam, ab14085), cells were washed by cold PBS and re-suspended in 500 μL of 1 × Binding Buffer. Then, 5 μL of Annexin V-FITC and 5 μL of propidium iodide were added into the Binding Buffer and incubated at room temperature for 5 min in the dark, and the stained cells were analyzed by flow cytometry.

2.6. Cell viability assay

Cytotoxicity of Cu^{2+} and chelators was evaluated by MTS assay. Briefly, after cells reached 80% confluence in 96-well plates, the cells were treated with Cu^{2+} or chelators for a suitable time. Then, 20 μL of CellTiter 96® AQueous One Solution Reagent (Promega, G3580) was added into each well of the 96-well assay plate containing the samples in 200 μL of culture medium. The MTS reagent was incubated with cells at 37 °C for 2 h, and then the absorbance at 490 nm was recorded by a SpectraMax M5 Microplate Reader. At the same time, every experimental groups subtracted the background absorbance of CellTiter 96® AQueous One Solution Reagent.

2.7. SOD1 activity assay

SOD1 activity was determined by measuring the inhibition of the reduction of the water-soluble tetrazolium salt, WST-1, which produced a water-soluble formazan dye upon reduction with O_2^-. The determinations were performed with a HT Superoxide Dismutase Assay Kit (Trevigen). Bovine SOD1 (Sigma), which has been proved to be equivalent to human SOD1, was used to generate a standard curve. After incubating 1 μM SOD1 with 0, 1, 5, 10, 30, 50 μM GT1 for 24 h at 37 °C, the activity of SOD1 was measured according to the manual.

3. Results and discussion

3.1. Design of hepatocyte-targeted copper chelators

In order to rationally design hepatocyte-targeted copper chelators based on the copper coordination chemistry and the recognition mechanism of ASGPR for galactose, several pivotal factors to be considered include: (1) the appropriate stability constants of the copper complexes, which cannot be much higher than the affinity constant of copper binding protein for copper ions, and so the $\log K_{Cu}^{2+}$ value of our chelators should be within the range of 11–17 (Banci et al., 2010); (2) the N-acetylgalactosamine or galactose-containing structure, which could be recognized by hepatocellular ASGPR; (3) the strong transmembrane ability, which allows both the chelators and the copper complexes in and out of the cells to increase the copper bioavailability.

Based on our experience in designing specific SOD1 inhibitors (Dong et al., 2016; Li et al., 2019), three Cu^{2+}-chelating agents were designed via a combination of phenol, thiosemicarbazone or semicarbazone, and lactobionic acid (Fig. 1, **GT1, 9 and 10**). The thiosemicarbazone and semicarbazone contain strongly copper-chelating and a H-bonding moiety —C(SH)—NH— and —C(OH)—NH—, respectively. The phenolic hydroxyl would modulate and facilitate the coordinating ability of thiosemicarbazone and semicarbazone to copper (Paterson and Donnelly, 2011). Finally, in order to achieve hepatocyte-targeted chelating agent delivery, lactobionic acid was covalently linked to the chelators, because galactose structure of lactobionic acid could be recognized by hepatocellular ASGPR.

The metal-coordinating moieties (**TH1, 9 and 10**) were synthesized by our previous procedures (Dong et al., 2016), and then the hepatocyte-targeted copper chelators containing lactobionic acid (**GT1, 9 and 10**) were synthesized according to Scheme S1. All compounds were fully characterized by NMR (^1H and ^{13}C) and MS in our ESI (Figs. S1–S18), which adequately demonstrated the accuracy of these compounds. As shown in Figs. S19a and S19c, lactobionic acid conjugation leaded to the disappearance of ν(—NH_2) characteristic peaks (**TH1**: 3289 cm^{-1}, **TH9**: 3344 cm^{-1}, **TH10**: 3352 cm^{-1}) in **GT1**, **GT9**, and **GT10**, which verified that lactobionic acid

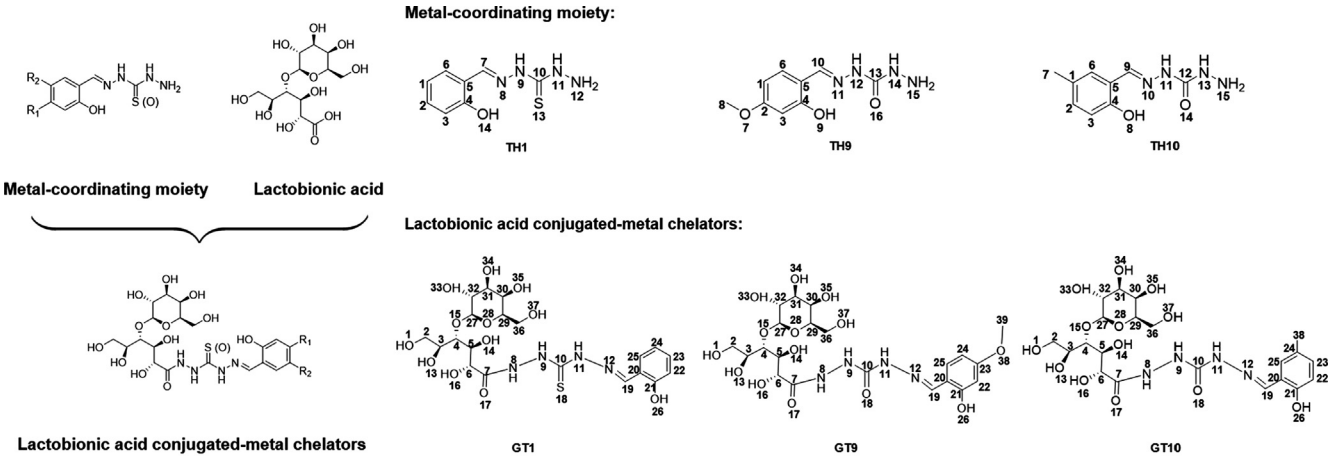

Fig. 1. The rational design of hepatocyte-targeted copper chelators. The design strategy of hepatocyte-targeted copper chelators through lactobionic acid conjugating.

was successfully covalently coupled to respective metal-coordinating moieties (Seleem et al., 2005; Shebl et al., 2010).

3.2. Coordination of chelators to copper

For the metal-coordinating moieties (**TH1, 9 and 10**) and copper chelators (**GT1, 9 and 10**), the stability constants of the complexes formed respectively with Cu^{2+}, Zn^{2+}, Mn^{2+} and Fe^{2+} were determined via potentiometric titrations at 25 °C. Considering the physical and chemical properties of trace elements similar to Cu^{2+} in human cells, Fe^{2+}, Zn^{2+} and Mn^{2+} are used for comparison in this work. As shown in Table 1, the binding capacities of each copper chelator and respective metal-coordinating moiety to copper are basically equal, such as **TH1** ($logK^{2+}_{Cu}$ = 17.82 ± 0.07) and **GT1** ($logK^{2+}_{Cu}$ = 17.48 ± 0.11), which indicated that the covalent linkage of lactobionic acid almost did not affect the binding of metal-coordinating moiety to copper. Compared with **GT9** and **10**, the chelator **GT1**, designed on the basis of thiosemicarbazone, has a much stronger binding ability with copper (Table 1). The higher ability of thiosemicarbazone to bind metal is also confirmed by our previous work, in which the thiosemicarbazone based chelator **LD18** have higher ability than semicarbazone based chelator **LD27** to bind metal (Dong et al., 2016). Under our testing conditions, both **GT1**, **9** and **10** have stronger binding ability to Cu^{2+} than Fe^{2+}, Zn^{2+} and Mn^{2+}, which implies that the chelators have notable selectivity for Cu^{2+} over the other divalent metal ions tested (Table 1). On the other hand, Peep Palumaa and the collaborators had indicated that the stability constants ($logK_{Cu}$) between copper and common copper-containing proteins are in the range of 14–17 (Banci et al., 2010). Therefore, our chelators would not interfere with the normal function of copper proteins in the cell, because the stability constants of copper complexes formed by **GT1**, **9** and **10** are not significantly higher than the intracellular copper-containing proteins (Table 1).

Next, solution speciation diagrams were calculated for the coordination of the metal-coordinating moieties and chelators to Cu^{2+}, Fe^{2+}, Zn^{2+} and Mn^{2+} (Fig. 2a and S20a) using the stability constants in Table 1. All of these diagrams indicated that the Cu^{2+}-chelator complexes are the predominant species formed in the range of pH 3–9 (Table 1). This pH range requisite for the formation of stable complexes completely covers the pH range of intracellular environment. In our previous work, the complexes had been confirmed by the crystal structures of the Cu^{2+} complexes formed with thiosemicarbazone and semicarbazone based chelators (Dong et al., 2016), whose metal-coordinating moieties are similar to **GT1**, **9** and **10**.

In order to further demonstrate the binding properties of the hepatocyte-targeted copper chelators toward copper ions, we also evaluated the interactions between Cu^{2+} and these chelators by spectrophotometric titrations. As shown in Fig. 2b, upon titration of Cu^{2+}, the intense absorption band at 345 nm (for **GT1**), 326 nm (for **GT9**) and 335 nm (for **GT10**) decreased gradually along with the increase of a new band at 395 nm (for **GT1**), 380 nm (for **GT9**) and 393 nm (for **GT10**), respectively. Furthermore, the well-defined isosbestic points at 370 nm (for **GT1**), 348 nm (for **GT9**) and 352 nm (for **GT10**) distinguished the free chelators and the respective copper complexes clearly (Fig. 2b). In physiology-like conditions (10% FBS), the characteristic absorption peaks of respective copper complexes at 395 nm (for **GT1**), 380 nm (for **GT9**) and 393 nm (for **GT10**) were also obtained upon titration of Cu^{2+} (Fig. S20b), which suggested that both **GT1**, **9** and **10** might coordinate with Cu^{2+} in physiology conditions. According to the results of potentiometric and spectrophotometric titrations, both **GT1**, **9** and **10** can preferentially bind to Cu^{2+} in vitro, and the binding capacity of **GT1** is slightly stronger than **GT9** and **10**. Furthermore, the results of infrared spectrum also confirmed the coordinating of cooper with chelators. The strong bands at 1618, 1630, and 1626 cm^{-1} assigned to ν(C═N) for **GT1**, **GT9** and **GT10**, respectively, were shifted to lower wave numbers (19–34 cm^{-1}) in copper complexes (Figs. S19b and S19c). These indicated the participation of the azomethine nitrogen in the chelation (Shebl et al., 2010; Chandra and Kumar, 2007; Sen et al., 2008). In copper complexes of **GT1**; **GT9** and **GT10**, the disappearance of ν(C═S) or ν(C═O) bands provided an evidence that the thiolic S or enolic O participate in the chelation after deprotonation leading to a covalent linkage (Singh and Singh, 2003). Therefore, our IR spectra of copper complexes are consistent with the IR results of

Table 1 The data for coordination with different divalent metal ions of the metal-coordinating moieties and chelators.

Ligand (K_M^{2+} value[1])	TH1	TH9	TH10	GT1	GT9	GT10
$\log K_{Cu}^{2+}$, n = 1, M^{-1}	17.82 ± 0.07	16.17 ± 0.03	15.91 ± 0.02	17.48 ± 0.11	15.59 ± 0.18	14.52 ± 0.20
$\log K_{Zn}^{2+}$, n = 1, M^{-1}	17.13 ± 0.05	15.28 ± 0.04	14.74 ± 0.09	15.90 ± 0.23	13.41 ± 0.18	12.83 ± 0.19
$\log K_{Mn}^{2+}$, n = 1, M^{-1}	14.11 ± 0.03	14.86 ± 0.11	14.29 ± 0.07	14.85 ± 0.04	12.45 ± 0.14	11.83 ± 0.18
$\log K_{Fe}^{2+}$, n = 1, M^{-1}	16.45 ± 0.05	14.34 ± 0.03	14.07 ± 0.06	15.10 ± 0.26	12.99 ± 0.41	12.32 ± 0.43
K_{Cu}^{2+}/K_{Zn}^{2+}	4.90	7.76	1.48×10^1	3.80×10^1	1.51×10^2	4.90×10^1
K_{Cu}^{2+}/K_{Mn}^{2+}	5.13×10^3	2.04×10^1	4.17×10^1	4.27×10^2	1.38×10^3	4.90×10^2
K_{Cu}^{2+}/K_{Fe}^{2+}	2.34×10^1	6.76×10^1	6.92×10^1	2.40×10^2	3.98×10^2	1.58×10^2
pH range[2]	3–9	3–9	3–9	3–9	3–9	3–9

[1] K_M^{2+} is the stability constant of metal ion and chelator, which is calculated from ML (metal–ligand).
[2] pH range indicates K_M^{2+} was calculated in pH 3–9.

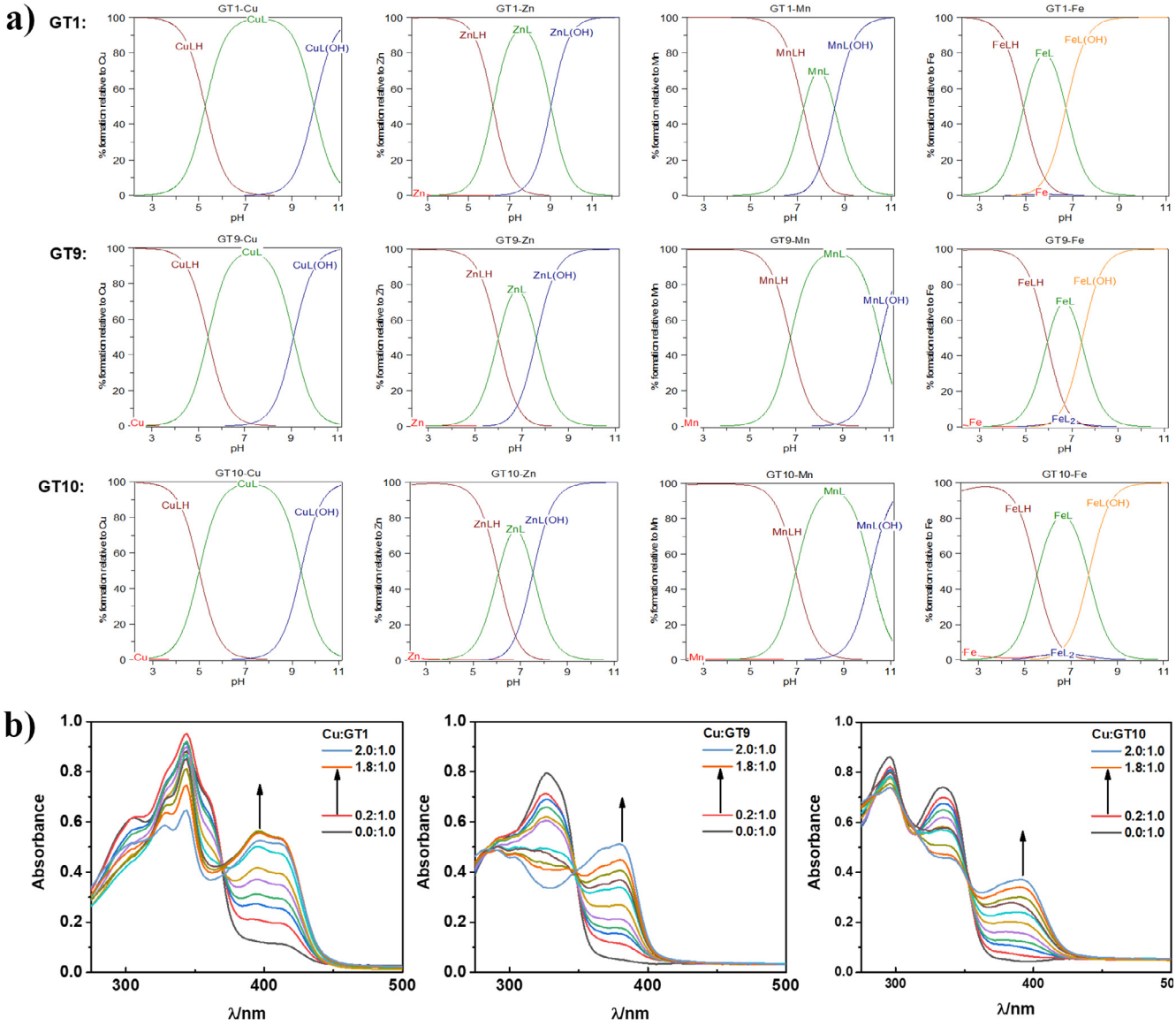

Fig. 2. The metal binding characterization of hepatocyte-targeted copper chelators. (**a**) Species distribution plots measured using potentiometric titrations for the Cu^{2+}, Zn^{2+}, Mn^{2+} and Fe^{2+}-chelator systems. The sources of Cu^{2+}, Zn^{2+}, Mn^{2+}, and Fe^{2+} are $CuCl_2$, $ZnCl_2$, $MnCl_2$ and $FeCl_2$, respectively. Potentiometric titrations were performed for the solutions containing the chelators and equimolar amounts of metal ions at 25 °C (I = 0.1 M KCl). (**b**) Spectrophotometric titrations of chelators (10 mM) with Cu^{2+} (0–20 mM) at 25 °C.

thiosemicarbazone- and semicarbazone-based copper complexes in the literature (Seleem et al., 2005; Shebl et al., 2010; Chandra and Kumar, 2007; Sen et al., 2008; Singh and Singh, 2003), and are also consistent with the single crystal structure of copper complexes in our previous work (Dong et al., 2016).

3.3. Construction of copper deposition cell model

Our results indicated that the chelators (**GT1**, **9** and **10**) could preferentially coordinate with copper, and the binding strength was also moderate. In order to systematically evaluate the removal of hepatocellular copper deposition by our chelators, we should first construct an appropriate cellular model of copper deposition. Thus, we detected the effects of incubation time on the survival of Cu^{2+} treated liver hepatocellular cells (HepG2). As the treatment time increases (0, 24, 48, 72 and 96 h), 100 μM Cu^{2+} could gradually reduce the cell viability of HepG2, and the treatment time over 48 h was more detrimental to the cell survival (Fig. 3a). Next, we further evaluated the dependence of HepG2 cytotoxicity on Cu^{2+} concentration. The cytotoxicity of HepG2 increased with the increase of Cu^{2+} concentration, and the cell survival rate was close to 85% when treated with 50 μM Cu^{2+} for 48 h (Fig. 3b). Finally, we evaluated the relative concentration of intracellular copper ions using commercial Cu^{2+} fluorescent probe, Rhodamine 6G hydrazide (CAS: 932013-08-6) (Dujols et al., 1997). After treating HepG2 cells with 50 μM Cu^{2+} for 48 h, the cells were washed with PBS, and then incubated with a 5 μM fluorescent probe for 1 h to characterize the intracellular Cu^{2+} contents. The results indicated that the fluorescence intensity of intracellular Cu^{2+} increased by approximate 11.5 times, which revealed the successful construction of high-copper cell model (Fig. 3c). In order to balance the copper concentration and survival rate, we treated HepG2 cells with 50 μM Cu^{2+} for 48 h to construct the high-copper treated hepatocellular carcinomas model (**HC HepG2**), which was used as copper deposition model for our subsequent studies.

3.4. Elimination of hepatocellular copper deposition

In order to determine the concentration of chelators used in intracellular experiments, we first measured the cytotoxicity of **GT1**, **9** and **10** in normal and **HC HepG2** cells. After constructing the high-copper cell model, the **HC HepG2** cells were incubated with chelators for another 24 h, and the relative viability was recorded using MTS tetrazolium compound, which could be bioreduced by cells into a colored formazan product (Mosmann, 1983). The results indicated that all chelators killed **HC HepG2** cells at low doses (5–50 μM), and **GT1** could cause cell death more efficiently. The treatment with 5 μM **GT1** killed ~65% of **HC HepG2** cells, whereas the cells treated with 5 μM **GT9** or **10** maintained >90% cell viability (Fig. 4a). Besides, both **GT1**, **9** and **10** did not significantly affect normal HepG2 cells survival, in the chelator concentration range of 0–50 μM (Figs. S20c). Obviously, all copper chelators designed here can kill high-copper treated hepatocellular carcinomas with high efficiency, and the lethality decreased in the order of **GT1** > **GT9** ~ **GT10**, which may be due to the stronger binding capacity of thiosemicarbazone contained **GT1** to copper. It is well known that thiosemicarbazone- and semicarbazone-based chelators have already been developed into important anti-cancer agents, which can kill a variety of cancer cells (Bai et al., 2021; Gan et al., 2014; Patole et al., 2004; Kalinowski et al., 2009). Our results that thiosemicarbazone-based chelator **GT1** can kill cancer cells more effectively is also consistent with many reported studies (Bai et al., 2021; Gan et al., 2014; Patole et al., 2004). For example, Bai et al. showed that thiosemicarbazone-based chelators ($IC_{50} \approx 2$–11 μM) could kill triple negative breast cancer MDA-MB-231 cells more effectively than semicarbazone-based drugs (Bai et al., 2021), which also confirmed the reliability of our results. Compared with **TH1**, **9** and **10**, chelators with lactobionic acid conjugation (**GT1**, **9** and **10**) could kill **HC HepG2** cells more effectively (Fig. S21a), which suggests that lactobionic acid conjugation can improve the targeting effect of chelators on hepatocytes.

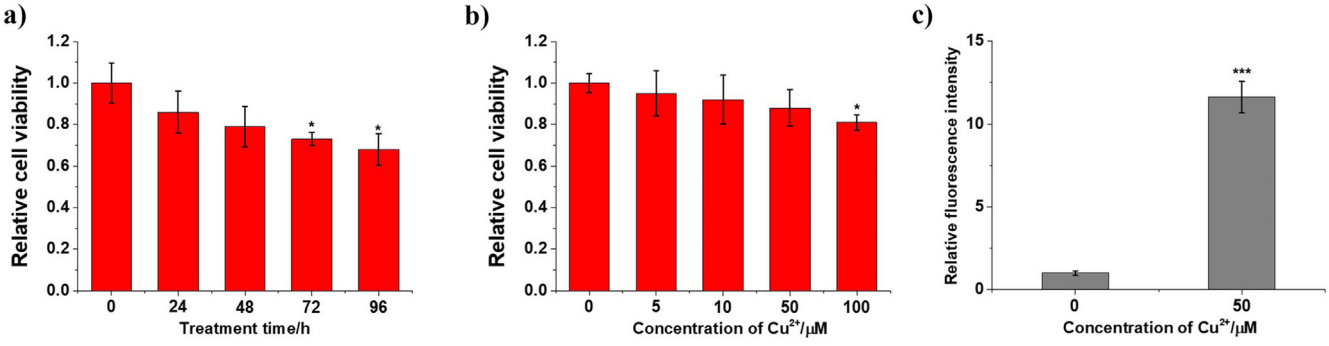

Fig. 3. Construction of high-copper treated hepatocellular carcinomas model (**HC HepG2** cells). (**a**) After incubating HepG2 cells with 100 μM Cu^{2+} for 0, 24, 48, 72 and 96 h, the cell viability was evaluated using commercial MTS kit. (**b**) After incubating HepG2 cells with 0, 5, 10 50 and 100 μM Cu^{2+} for 48 h, the cell viability was evaluated using commercial MTS kit. (**c**) The HepG2 cells were incubated with 50 μM Cu^{2+} for 48 h, washed with PBS three times, and then treated with 5 μM Cu^{2+} fluorescent probe (Rhodamine 6G hydrazide) for another 1 h to characterize the intracellular Cu^{2+} contents. All experiments were normalized by respective control data. Data are mean of triplicate samples ± SD (*$P < 0.05$, **$P < 0.01$, ***$P < 0.001$; unpaired Student's t test), and all error bars are SD.

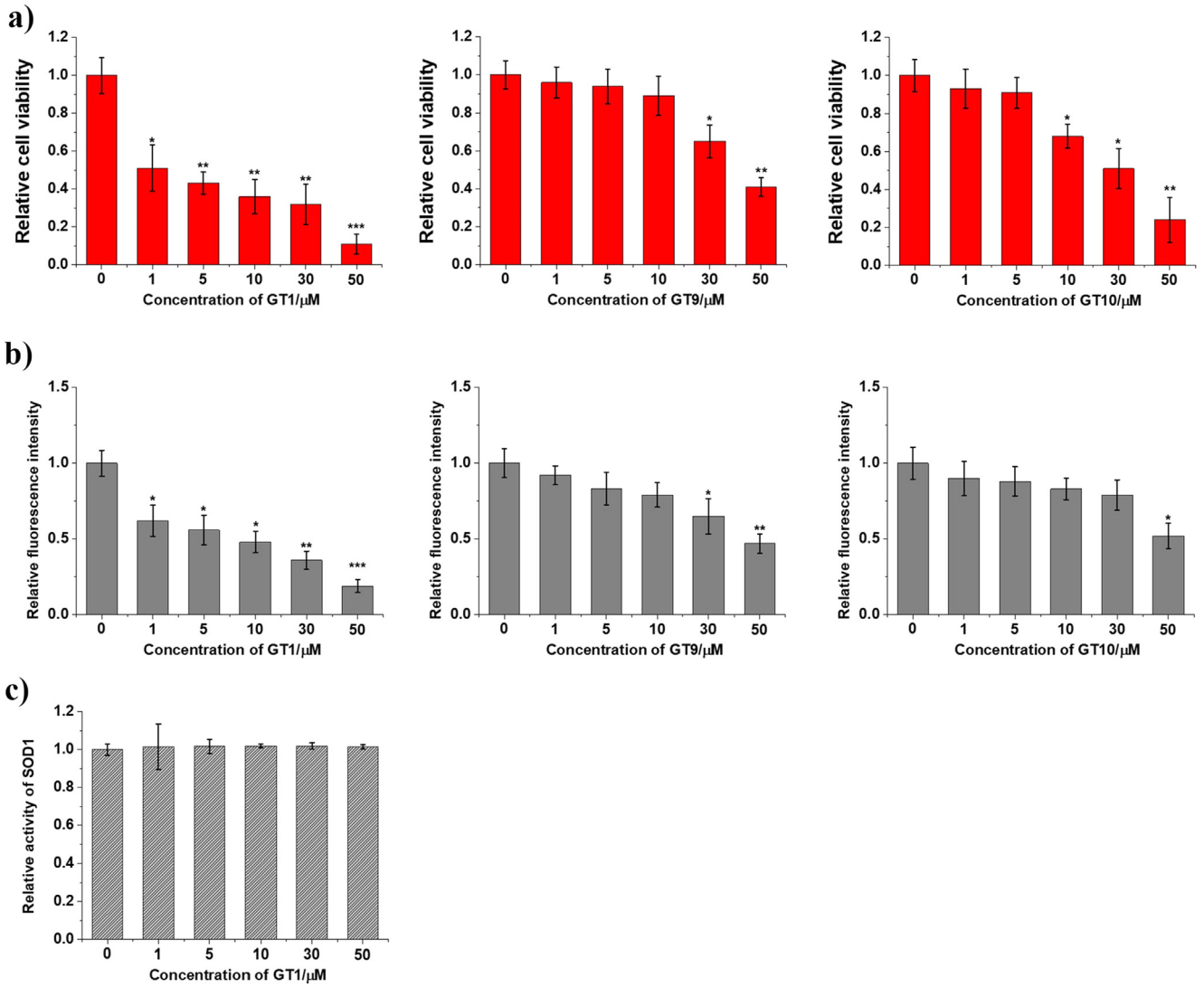

Fig. 4. Elimination of the hepatocellular copper deposition by chelators. After constructing the high-copper cell model, the **HC HepG2** cells were incubated with 0, 1, 5, 10, 30 and 50 μM chelators (**GT1**, **9** and **10**) for another 24 h. Then, the cell viability and intracellular Cu^{2+} contents were evaluated using commercial MTS kit (**a**) and Cu^{2+} fluorescent probe (**b**), respectively. SOD1 (1 μM) was incubated with 0, 1, 5, 10, 30, 50 μM **GT1** for 24 h at 37 °C, and then the activity of SOD1 was measured by commercial kit (**c**). For chelator treatment, the same amount of DMSO (5‰) was added as a control group, because DMSO was used as a co-solvent. All experiments were normalized by respective control data. Data are mean of triplicate samples ± SD (*$P < 0.05$, **$P < 0.01$, ***$P < 0.001$; unpaired Student's t test), and all error bars are SD.

Then, we systematically evaluated the effects of **GT1**, **9** and **10** on copper elimination in **HC HepG2** cells. The cells were incubated with different concentrations of **GT1**, **9** and **10** for 24 h, and then the relative copper content was detected using Rhodamine 6G hydrazide. For all chelators, the intracellular copper content of **HC HepG2** cells gradually decreased as the concentration increases of **GT1**, **9** and **10**. Consistent with the results in vitro, **GT1** also has better elimination effects on copper in **HC HepG2** cells (Fig. 4b). Respectively, 5 and 50 μM **GT1** drastically eliminated ~45% and ~80% intracellular copper. For **GT9** and **10**, 50 μM chelator eliminated only ~50% intracellular copper. However, 50 μM **GT1** only slightly eliminated ~15% and ~20% intracellular copper in high-copper treated HeLa and MCF-7 cells, which suggested that **GT1** could selectively eliminate copper for hepatocytes (Fig. S21b). Overall, our results suggested that **GT1** can eliminate copper deposition in hepatocellular carcinomas more efficiently, which might help us control the deterioration of hepatocytes or kill the copper-deposited hepatocellular carcinomas.

Because the stability constants ($\log K_{Cu}$) between copper and common copper-containing proteins are in the range of 14 to 17 (Banci et al., 2010); **GT1**, **9** and **10** should not interfere with the normal function of copper proteins (Table 1). To verify this hypothesis, we determined whether the chelator would inhibit the activity of copper/zinc superoxide dismutase (SOD1) using commercial kit. Our results reliably indicated that **GT1** will not interfere with the catalytic activity of SOD1 (Fig. 4c). In general, the chelators we designed can effectively eliminate copper deposition in hepatocellular carci-

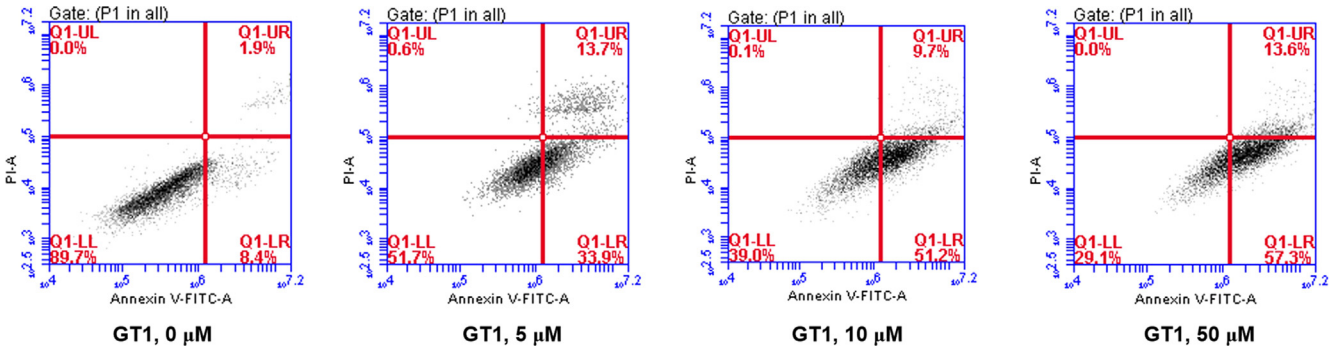

Fig. 5. Promotion of copper-deposited hepatocellular carcinomas apoptosis by **GT1**. After constructing the high-copper cell model, the **HC HepG2** cells were incubated with 0, 5, 10 and 50 μM **GT1** for another 24 h. For chelator treatment, the same amount of DMSO (5‰) was added as a control group, because DMSO was used as a co-solvent. Flow cytometric analysis of cell apoptosis was carried out with Annexin V and propidium iodide staining.

nomas, and will not affect the function of copper proteins. Among them, **GT1** has the best performance, which can strongly bind with Cu^{2+} and successfully kill **HC HepG2** cells at low doses.

3.5. Promotion of copper-deposited hepatocellular carcinomas apoptosis

The effect of **GT1** on copper-deposited hepatocellular carcinomas apoptosis was observed via flow cytometry, because the elimination of copper is not conducive to the survival of **HC HepG2** cells. The data showed that the **HC HepG2** cells display a drastically elevation in apoptosis following exposure to **GT1** for 24 h (Fig. 5). In detail, 5 μM **GT1** promoted 33.9% of **HC HepG2** cells to undergo apoptosis, and 10–50 μM **GT1** increased the proportion of apoptotic cells to even more than 50%. As shown in Fig. S22a, 50 μM **GT1** only promoted 15.9% of normal HepG2 cells to undergo apoptosis. These results indicated that eliminating the deposited copper in liver cancer cells can more effectively promote apoptosis, thereby killing such hepatocarcinoma cells. Earlier literature data also indicated that thiosemicarbazone-based metal chelator could cause a significant increasing in the population of apoptotic and dead cells (Bai et al., 2021). Therefore, both our results and literature data have shown that thiosemicarbazone-based metal chelator can kill cancer cells by promoting apoptosis. Furthermore, 50 μM **GT1** only caused both apoptosis and death of 16.5% MCF-10A cells (human normal mammary epithelial cells), which indicated that **GT1** has relatively small effects on non-cancerous cells (Fig. S22b).

The chelator **GT1** was designed via a combination of phenol, thiosemicarbazone, and lactobionic acid (Fig. 1). The use of thiosemicarbazone group enables **GT1** to have suitable binding capacity with copper ($\log K_{Cu}^{2+} = 17.48 \pm 0.11$). While effectively removing the copper deposits of hepatocarcinoma cells, it will not interfere with the functions of other copper proteins (Fig. 4b and 4c). Besides, lactobionic acid group of **GT1** can theoretically be recognized by hepatocellular ASGPR, which is expected to achieve hepatocyte-targeted chelating agent delivery. Because copper deposition is an important induction factor of hepatic carcinoma, **GT1** may have application prospects in intervening copper deposition and cancerization of liver. For the copper-deposited cells that have already undergone cancerous transformation, **GT1** can also promote cell apoptosis by chelating copper, thereby killing the cells (Figs. 4 and 5).

4. Conclusions

In this study, three specific and efficient copper chelators (**GT1**, **9** and **10**) were designed through combining copper-coordinating group, phenol, and lactobionic acid. Among them, **GT1** has the strongest binding capacity with copper, and can effectively chelate Cu^{2+} in the solution and in the cell. Through eliminating the intracellular copper, **GT1** facilitates the apoptosis and death of **HC HepG2** cells, a model of copper-deposited hepatocarcinoma cells. Due to its moderate copper-coordinating ability, **GT1** will not interfere with the normal function of intracellular copper proteins, such as SOD1. Besides, the conjugation of lactobionic acid has the potential to achieve hepatic targeting delivery of chelators through ASGPR. Therefore, **GT1** may have important application prospects in hepatic targeting copper elimination, which might be a potential method to inhibit copper-related cancerization of liver.

Declaration of Competing Interest

The authors declare that they have no known competing financial interests or personal relationships that could have appeared to influence the work reported in this paper.

Acknowledgements

This work was supported by the National Natural Science Foundation of China [21701128]; Hubei Provincial Natural Science Foundation of China [2017CFB206]; Educational Commission of Hubei Province of China [Q20171601].

Appendix A. Supplementary material

Supplementary data to this article can be found online at https://doi.org/10.1016/j.arabjc.2021.103241.

References

Alderighi, L., Gans, P., Ienco, A., Peters, D., Sabatini, A., Vacca, A., 1999. Hyperquad simulation and speciation (HySS): a utility program for the investigation of equilibria involving soluble and partially soluble species. Coord. Chem. Rev. 184, 311–318.

Aruoma, O.I., Halliwell, B., Gajewski, E., Dizdaroglu, M., 1991. Copper-ion-dependent damage to the bases in DNA in the presence of hydrogen peroxide. Biochem. J. 273, 601–604.

Bai, C., Wu, S., Ren, S., Zhu, M., Luo, G., Xiang, H., 2021. Synthesis and evaluation of novel thiosemicarbazone and semicarbazone analogs with both anti-proliferative and anti-metastatic activities against triple negative breast cancer. Bioorg. Med. Chem. 37, 116107.

Banci, L., Bertini, I., Ciofi-Baffoni, S., Kozyreva, T., Zovo, K., Palumaa, P., 2010. Affinity gradients drive copper to cellular destina-tions. Nature 465, 645–648.

Bandmann, O., Weiss, K.H., Kaler, S.G., 2015. Wilson's disease and other neurological copper disorders. Lancet. Neurol. 14, 103–113.

Bernardes, G.J., Kikkeri, R., Maglinao, M., Laurino, P., Collot, M., Hong, S.Y., Lepenies, B., Seeberger, P.H., 2010. Design, synthesis and biological evaluation of carbohydrate-functionalized cyclodextrins and liposomes for hepatocyte-specific targeting. Org. Biomol. Chem. 8, 4987–4996.

Brady, D.C., Crowe, M.S., Turski, M.L., Hobbs, G.A., Yao, X., Chaikuad, A., Knapp, S., Xiao, K., Campbell, S.L., Thiele, D.J., et al, 2014. Copper is required for oncogenic BRAF signalling and tumorigenesis. Nature 509, 492–496.

Bruix, J., Boix, L., Sala, M., Llovet, J.M., 2004. Focus on hepatocellular carcinoma. Cancer Cell 5, 215–219.

Chandan, V.S., Shah, S.S., Mounajjed, T., Torbenson, M.S., Wu, T. T., 2018. Copper deposition in focal nodular hyperplasia and inflammatory hepatocellular adenoma. J. Clin. Pathol. 71, 504–507.

Chandra, S., Kumar, A., 2007. Spectroscopic evaluation of Co(II), Ni (II) and Cu(II) complexes derived from thiosemicarbazone and semicarbazone. Spectrochim. Acta A 68, 1410–1415.

Crouch, P.J., Hung, L.W., Adlard, P.A., Cortes, M., Lal, V., Filiz, G., Perez, K.A., Nurjono, M., Caragounis, A., Du, T., et al, 2009. Increasing Cu bioavailability inhibits Abeta oligomers and tau phosphorylation. PNAS 106, 381–386.

Członkowska, A., Litwin, T., Dusek, P., Ferenci, P., Lutsenko, S., Medici, V., Rybakowski, J.K., Weiss, K.H., Schilsky, M.L., 2018. Wilson disease. Nat. Rev. Dis. Primers 4, 1–20.

Daniel, K.G., Harbach, R.H., Guida, W.C., Dou, Q.P., 2004. Copper storage diseases: Menkes, Wilsons, and cancer. Front. Biosci. 9, 2652–2662.

Danks, D.M., 1991. Copper and liver disease. Eur. J. Pediatr. 150, 142–148.

Dong, X., Zhang, Z., Zhao, J., Lei, J., Chen, Y., Li, X., Chen, H., Tian, J., Zhang, D., Liu, C., Liu, C., 2016. The rational design of spe-cific SOD1 inhibitors via copper coordination and their application in ROS signaling research. Chem. Sci. 7, 6251–6262.

Dujols, V., Ford, F., Czarnik, A.W., 1997. A long-wavelength fluorescent chemodosimeter selective for Cu(II) ion in water. J. Am. Chem. Soc. 119, 7386–7387.

Gan, C., Cui, J., Su, S., Lin, Q., Jia, L., Fan, L., Huang, Y., 2014. Synthesis and antiproliferative activity of some steroidal thiosemicarbazones, semicarbazones and hydrozones. Steroids 87, 99–107.

Gans, P., Sabatini, A., Vacca, A., 1996. Investigation of equilibria in solution. Determination of equilibrium constants with the HYPERQUAD suite of programs. Talanta 43, 1739–1753.

Gans, P., Sabatini, A., Vacca, A., 1999. Determination of equilibrium constants from spectrophometric data obtained from solutions of known pH: the program pHab. Ann. Chim 89, 45–49.

Gupte, A., Mumper, R.J., 2009. Elevated copper and oxidative stress in cancer cells as a target for cancer treatment. Cancer Treat. Rev. 35, 32–46.

Harris, E.D., 2001. Copper homeostasis: the role of cellular transporters. Nutr. Rev. 59, 281–285.

Huang, X., Leroux, J.C., Castagner, B., 2017. Well-defined multivalent ligands for hepatocytes targeting via asialoglycoprotein receptor. Bioconjug. Chem. 28, 283–295.

Hussain, S.P., Hofseth, L.J., Harris, C.C., 2003. Radical causes of cancer. Nat. Rev. Cancer 3, 276–285.

Hussain, S.P., Schwank, J., Staib, F., Wang, X.W., Harris, C.C., 2007. TP53 mutations and hepatocellular carcinoma: insights into the etiology and pathogenesis of liver cancer. Oncogene 26, 2166–2176.

Johncilla, M., Mitchell, K.A., 2011. Pathology of the liver in copper overload. Semin. Liver Dis. 31, 239–244.

Kacar, S., Unver, H., Sahinturk, V., 2020. A mononuclear copper(II) complex containing benzimidazole and pyridyl ligands: Syn-thesis, characterization, and antiproliferative activity against human cancer cells. Arab. J. Chem. 13, 4310–4323.

Kalinowski, D.S., Quach, P., Richardson, D.R., 2009. Thiosemicarbazones: the new wave in cancer treatment. Future Med. Chem. 1, 1143–1151.

Kim, B.E., Nevitt, T., Thiele, D.J., 2008. Mechanisms for copper acquisition, distribution and regulation. Nat. Chem. Biol. 4, 176–185.

Krasnovskaya, O.O., Fedorov, Y.V., Gerasimov, V.M., Skvortsov, D. A., Moiseeva, A.A., Mironov, A.V., Beloglazkina, E.K., Zyk, N. V., Majouga, A.G., 2016. Novel 2-aminoimidazole-4-one complexes of copper(ii) and cobalt(ii): synthesis, structural characterization and cytotoxicity. Arab. J. Chem. 12, 835–846.

Li, X., Chen, Y., Zhao, J., Shi, J., Wang, M., Qiu, S., Hu, Y., Xu, Y., Cui, Y., Liu, C., Liu, C., 2019. The specific inhibition of SOD1 selectively promotes apoptosis of cancer cells via regulation of the ROS signaling network. Oxid. Med. Cell. Longev. 2019, 1–21.

Li, Y,; Huang, G,; Diakur, J,; Wiebe, L. Targeted delivery of macromolecular drugs: asialoglycoprotein receptor (ASGPR) expression by selected hepatoma cell lines used in antiviral drug development. Curr. Drug Deliv. 2008, 5, 299-302.

Mamidyala, S.K., Dutta, S., Chrunyk, B.A., Préville, C., Wang, H., Withka, J.M., McColl, A., Subashi, T.A., Hawrylik, S.J., Griffor, M.C., et al, 2012. Glycomimetic ligands for the human asialoglycoprotein receptor. J. Am. Chem. Soc. 134, 1978–1981.

Merlot, A.M., Kalinowski, D.S., Richardson, D.R., 2013. Novel chelators for cancer treatment: where are we now? Antioxid. Redox Signal. 18, 973–1006.

Mosmann, T., 1983. Rapid colorimetric assay for cellular growth and survival: application to proliferation and cytotoxicity assays. J. Immunol. Methods 65, 55–63.

Paterson, B.M., Donnelly, P.S., 2011. Copper complexes of bis (thiosemicarbazones): from chemotherapeutics to diagnostic and therapeutic radiopharmaceuticals. Chem. Soc. Rev. 40, 3005–3018.

Patole, J., Padhye, S., Newton, C., Anson, C., Powell, A.K., 2004. Synthesis, characterization and in vitro anti-cancer activities of semicarbazone and thio-semicarbazone derivatives of salic-ylaldehyde and their copper complexes against human breast cancer cell line MCF-7. Indian J. Chem. 43, 1654–1658.

Paulsen, C.E., Carroll, K.S., 2013. Cysteine-mediated redox signaling: chemistry, biology, and tools for discovery. Chem. Rev. 113, 4633–4679.

Porchia, M., Tisato, F., Zancato, M., Gandin, V., Marzano, C., 2020. In vitro antitumor activity of water-soluble copper(I) complexes with diimine and monodentate phosphine ligands. Arab. J. Chem. 13, 998–1010.

Pujol, A.M., Cuillel, M., Renaudet, O., Lebrun, C., Charbonnier, P., Cassio, D., Gateau, C., Dumy, P., Mintz, E., Delangle, P., 2011. Hepatocyte targeting and intracellular copper chelation by a thiol-containing glycocyclopeptide. J. Am. Chem. Soc. 133, 286–296.

Rigopoulou, E.I., Roggenbuck, D., Smyk, D.S., Liaskos, C., Mytilinaiou, M.G., Feist, E., Conrad, K., Bogdanos, D.P., 2012. Asialoglycoprotein receptor (ASGPR) as target autoantigen in liver autoimmunity: lost and found. Autoimmun. Rev. 12, 260–269.

Roberts, E.A., Sarkar, B., 2008. Liver as a key organ in the supply, storage, and excretion of copper. Am. J. Clin. Nutr. 88, 851S–854S.

Safi, R., Nelson, E.R., Chitneni, S.K., Franz, K.J., George, D.J., Zalutsky, M.R., McDonnell, D.P., 2014. Copper signaling axis as a target for prostate cancer therapeutics. Cancer Res. 74, 5819–5831.

Sanhueza, C.A., Baksh, M.M., Thuma, B., Roy, M.D., Dutta, S., Préville, C., Chrunyk, B.A., Beaumont, K., Dullea, R., Am-mirati, M., et al, 2017. Efficient liver targeting by polyvalent display of a compact ligand for the asialoglycoprotein receptor. J. Am. Chem. Soc. 139, 3528–3536.

Santini, C., Pellei, M., Gandin, V., Porchia, M., Tisato, F., Marzano, C., 2014. Advances in copper complexes as anticancer agents. Chem. Rev. 114, 815–862.

Seleem, H.S., El-Shetary, B.A., Khalil, S.M.E., Mostafa, M., Shebl, M., 2005. Structural diversity in copper(II) complexes of bis (thiosemicarbazone) and bis(semicarbazone) ligands. J. Coord. Chem. 58, 479–493.

Sen, S., Shit, S., Mitra, S., Batten, S.R., 2008. Structural and spectral studies of a new copper(II) complex with a tridentate thiosemicarbazone ligand. Struct. Chem. 19, 137–142.

Shebl, M., Seleem, H.S., El-Shetary, B.A., 2010. Ligational behavior of thiosemicarbazone, semicarbazone and thiocarbohydrazone ligands towards VO(IV), Ce(III), Th(IV) and UO2(VI) ions: synthesis, structural characterization and biological studies. Spectrochim. Acta A 75, 428–436.

Singh, M.S., Singh, P.K., 2003. Highly versatile synthesis of some organotin(IV) complexes of 2-Hydroxyacetophenone semicarbazone and thiosemicarbazone. Syn. React. Inorg. Met. 33, 1895–1909.

Smallwood, R.A., Williams, H.A., Rosenoer, V.M., Sherlock, S., 1968. Liver-copper levels in liver disease: studies using neutron activation analysis. Lancet 2, 1310–1313.

Stepien, M., Hughes, D.J., Hybsier, S., Bamia, C., Tjønneland, A., Overvad, K., Affret, A., His, M., Boutron-Ruault, M.C., Katzke, V., et al, 2017. Circulating copper and zinc levels and risk of hepatobiliary cancers in Europeans. Br. J. Cancer 116, 688–696.

Theophanides, T., Anastassopoulou, J., 2002. Copper and carcinogenesis. Crit. Rev. Oncol. Hematol. 42, 57–64.

Thomas, J.A., Buchsbaum, R.N., Zimniak, A., Racker, E., 1979. Intracellular pH measurements in Ehrlich ascites tumor cells utilizing spectroscopic probes generated in situ. Biochemistry 18, 2210–2218.

Turski, M.L., Brady, D.C., Kim, H.J., Kim, B.E., Nose, Y., Counter, C.M., Winge, D.R., Thiele, D.J., 2012. A novel role for copper in Ras/mitogen-activated protein kinase signalling. Mol. Cell Biol. 32, 1284–1295.

Ueda, K., Matsui, O., Nakanumai, Y., Terada, T., Kadoya, M., Kitagawa, K., Kobayashi, S., Kawamori, Y., Gabata, T., Takashima, T., 1993. Deposition of copper and copper-binding protein (CBP) in adenomatous hyperplasia of the liver: relevance to magnetic resonance imaging. Int. Hepatol. Commun. 1, 326–330.

Wang, J., Luo, C., Shan, C., You, Q., Lu, J., Elf, S., Zhou, Y., Wen, Y., Vinkenborg, J.L., Fan, J., et al, 2015. Inhibition of human copper trafficking by a small molecule significantly attenuates cancer cell proliferation. Nat. Chem. 7, 968–979.

Williams, D.M., 1983. Copper deficiency in humans. Semin. Hematol. 20, 118–128.

Wooton-Kee, C.R., Jain, A.K., Wagner, M., Grusak, M.A., Finegold, M.J., Lutsenko, S., Moore, D.D., 2015. Elevated copper impairs hepatic nuclear receptor function in Wilson's disease. J. Clin. Invest. 125, 3449–3460.

Yoshii, J., Yoshiji, H., Kuriyama, S., Ikenaka, Y., Noguchi, R., Okuda, H., Tsujinoue, H., Nakatani, T., Kishida, H., Dai, N., 2001. The copper-chelating agent, trientine, suppresses tumor development and angiogenesis in the murine hepatocellular carcinoma cells. Int. J. Cancer 94, 768–773.

Zubair, H., Khan, H.Y., Sohail, A., Azim, S., Ullah, M.F., Ahmad, A., Sarkar, F.H., Hadi, S.M., 2013. Redox cycling of endogenous copper by thymoquinone leads to ROS-mediated DNA breakage and consequent cell death: putative anticancer mechanism of antioxidant. Cell Death Dis. 4, e660–e667.